

# Periodicity-Doubling Cascades: Direct Observation in Ferroelastic Materials

Arnoud S. Everhardt,<sup>1,\*</sup> Silvia Damerio,<sup>1,†</sup> Jacob A. Zorn,<sup>2</sup> Silang Zhou,<sup>1</sup> Neus Domingo,<sup>3</sup> Gustau Catalan,<sup>3,4</sup>  
Ekhard K. H. Salje,<sup>5</sup> Long-Qing Chen,<sup>2</sup> and Beatriz Noheda<sup>1,6,‡</sup>

<sup>1</sup>*Zernike Institute for Advanced Materials, University of Groningen, 9747AG- Groningen, Netherlands*

<sup>2</sup>*Department of Materials Science and Engineering, The Pennsylvania State University,  
University Park, Pennsylvania 16802, USA*

<sup>3</sup>*Catalan Institute of Nanoscience and Nanotechnology (ICN2), 08193 Barcelona, Catalonia, Spain*

<sup>4</sup>*ICREA, 08193 Barcelona, Catalonia, Spain*

<sup>5</sup>*University of Cambridge, Cambridge, Oxford OX1 3AN, United Kingdom*

<sup>6</sup>*CogniGron Center, University of Groningen, 9747AG- Groningen, Netherlands*



(Received 29 January 2019; revised manuscript received 6 May 2019; published 22 August 2019)

Very sensitive responses to external forces are found near phase transitions. However, transition dynamics and preequilibrium phenomena are difficult to detect and control. We have observed that the equilibrium domain structure following a phase transition in ferroelectric and ferroelastic BaTiO<sub>3</sub> is attained by halving of the domain periodicity multiple times. The process is reversible, with periodicity doubling as temperature is increased. This observation is reminiscent of the period-doubling cascades generally observed during bifurcation phenomena, and, thus, it conforms to the “spatial chaos” regime earlier proposed by Jensen and Bak [*Phys. Scr. T* **9**, 64 (1985)] for systems with competing spatial modulations.

DOI: [10.1103/PhysRevLett.123.087603](https://doi.org/10.1103/PhysRevLett.123.087603)

Current interest in adaptable electronics calls for new paradigms of material systems with multiple metastable states. Functional materials with modulated phases bring interesting possibilities in this direction [1]. Ferroic materials are good prospective candidates because the modulation can be controlled by external magnetic, electric, or stress fields. In magnetic materials, the presence of competing interactions can lead to a wealth of modulated structures, exemplified by the axial next-nearest-neighbor Ising model [2]. In ferroelectrics, interesting modulations in the form of domain patterns involve not only domains with alternating up and down polarization but also vortices [3] and ferroelectric skyrmions [4]. Ferroelectrics are often also ferroelastic [5] and display modulations of the strain.

When ferroelastic materials are grown in thin film form on a suitable crystalline substrate, they can be subjected to epitaxial strain, which typically relaxes by the formation of ferroelastic domains [6,7]. In the simple case of ferroelastic systems with orthogonal lattices grown on a cubic substrate, different types of 90° domain configurations form, either so-called *a/c* domains (with the long *c* axis alternating in plane and out of plane) or *a/b* domains (long axis, fully in plane), depending on the sign of the strain imposed on the film by the substrate [8]. In the absence of dislocations or other defects, ferroelastic domains in epitaxial films are expected to alternate periodically [6–8].

The periodicity of this modulation, or the domain width (*w*), is determined by the competition between the elastic energy in the domains and the formation energy of domain

walls and is a function of the thin film thickness (*d*). For *d* > *w*, the relation  $w = \beta d^{1/2}$  holds, as a particular case of Kittel's law [6,9–11]. In the ferroelastic case, geometrical effects are also important and discretization of domain widths, with minimum sizes determined by the need for lateral lattice coherence at the domain wall, have also been shown [12,13]. Recently, an original hydrodynamicslike approach has been put forward, in which nonequilibrium ferroic domain structures are rationalized with respect to surface folding, wrinkling, and relaxation [14].

As both misfit strain and domain wall energies change with temperature, the equilibrium patterns are temperature dependent, and the question arises of how does the system evolves towards (global or local) equilibrium. While studies of ferroelectric domain formation and switching are common [15–20], less attention has been paid to microscopy studies of temperature-driven annihilation of ferroelastic nanodomains [21,22] and it is only recently that experimental developments have allowed the *in situ* study of domain dynamics [23–28].

In this Letter, we report on the direct observation of ferroelastic and ferroelectric domain evolution by sequential periodicity halving and doubling on BaTiO<sub>3</sub> thin films. Moreover, we present the results of phase-field simulations [29–32] that support the observations showing that domain wall nucleation takes place in the center of existing domains. Period-doubling cascades, associated with the proximity of order-to-chaos transitions, have often been observed as frequency doubling sequences in the time

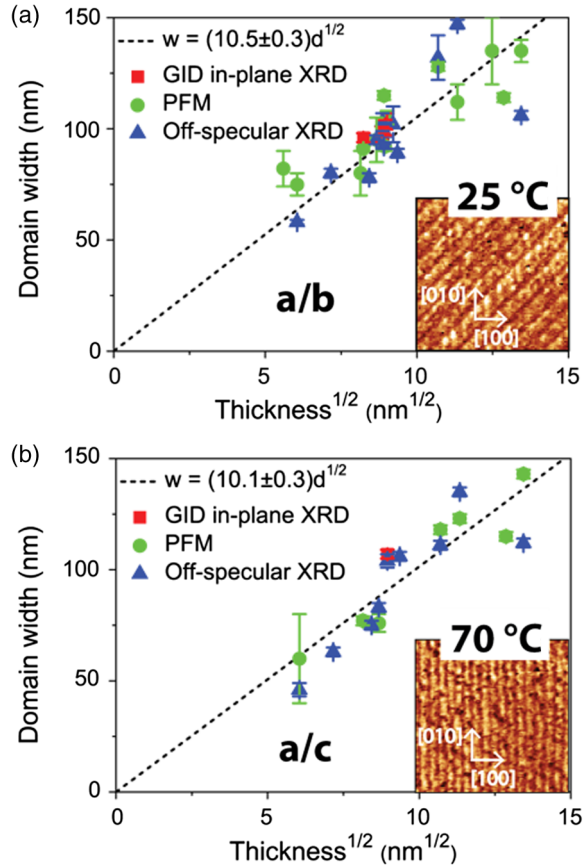


FIG. 1. Domain widths for different film thicknesses, determined by grazing incidence diffraction (GID) XRD, off-specular XRD around the (204) Bragg peaks or PFM (see Ref. [33]). The data are fitted to a square-root law with parameter  $\beta$  shown in the legend for the (a)  $a/b$  and (b)  $a/c$  domain states. (Insets) Amplitude LPM images of a 80 nm thick BaTiO<sub>3</sub> film at (a) 25 °C and (b) 70 °C. The images are of a  $1 \times 1 \mu\text{m}$  area with edges along [100] and [010].

regime, but they have not yet been reported in spatially modulated systems. The results, thus, present strong evidence that ferroelastic systems with competing modulations are at the edge of chaos, as predicted for magnetic materials by Jensen and Bak [1].

The experiments have been performed on BaTiO<sub>3</sub> films grown under low epitaxial strain on SrRuO<sub>3</sub>-buffered NdScO<sub>3</sub> substrates, as described in Ref. [33]. The low-strain condition flattens the energy landscape such that different ferroelectric domain configurations can be accessed within a moderate temperature range [34]. In particular, the films display a paraelectric-ferroelectric phase transition at 130 °C, and a second transition at about 50 °C. The latter takes place between two quite complex ferroelectric and ferroelastic phases (see Sec. I of the Supplemental Material [35] for details), but, for the sake of clarity, it can simply be described as a transition from a high-temperature, pseudotetragonal  $a/c$  domain structure to a low-temperature, pseudo-orthorhombic  $a/b$

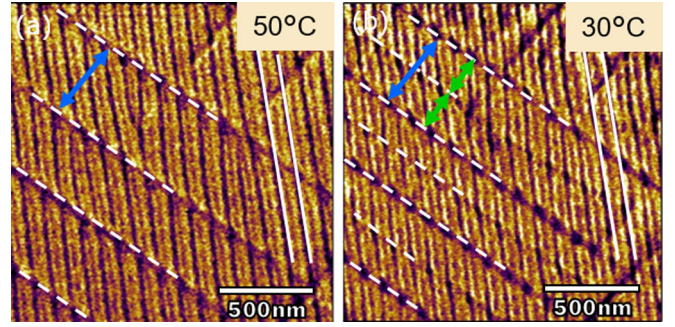


FIG. 2. Amplitude lateral PFM (LPM) images of a 170 nm thick BaTiO<sub>3</sub> film on a NdScO<sub>3</sub> substrate. The transition from  $a/c$  to  $a/b$  domains is followed on cooling and images are shown in the coexistence regime at (a) 50 °C and (b) 30 °C. The dashed lines indicate the  $a/b$  domain walls, whose in-plane projections are parallel to the  $[\bar{1}10]$  direction; while the solid lines indicate two  $a/c$  domain walls, with in-plane projection parallel to the [010] direction. The blue double arrows signal the initial periodicity of  $w_0 \sim 500$  nm. At 30 °C, new  $a/b$  domains appear in the center of the existing domains. The green double arrows in (b) indicate the observed  $a/b$  domains with  $w = 0.5w_0 \sim 250$  nm.

domain structure [51]. Unlike in other ferroics, the transformation from  $a/c$  to  $a/b$  domains in these films is slow enough to be followed with piezoresponse force microscopy (PFM) (see Sec. II of the Supplemental Material [35] for details).

Typical domain configurations below and above the transition can be seen in the insets of Figs. 1(a) and 1(b), at 25 °C and 70 °C, respectively. The inset in Fig. 1(a) shows  $a/b$  domains with domain wall projections parallel to the [110] direction. The inset in Fig. 1(b) shows  $a/c$  domain walls with projections parallel to the [010] direction. Investigation of a large number of samples with thicknesses ranging from 30 to 330 nm confirms the robustness of the domain configurations and the expected  $w = \beta d^{1/2}$  scaling law, with  $\beta \sim 10 \text{ nm}^{1/2}$  for both the  $a/b$  and  $a/c$  domains, as shown in Fig. 1. Here, the  $a/c$  structure refers to the domains generated while cooling from the paraelectric phase. When the  $a/c$  domain configuration is reached upon heating from the low-temperature  $a/b$  configuration,  $\beta$  is reduced to  $\sim 7 \text{ nm}^{1/2}$ , reflecting the important role of preexisting domain walls in the nucleation of new domain walls (see Sec. III of the Supplemental Material [35] for details).

In order to investigate the evolution of the domain formation, the films were heated to 200 °C and measured during cooling. During the cooldown process, the  $a/c$  structure arises below the paraelectric-ferroelectric transition. At a temperature of 70 °C, the first  $b$  domains start appearing inside the  $a/c$  matrix, and increasing in number as the temperature lowers. Figure 2 shows images of two stages of the domain evolution taken while cooling with 5 °C steps. At 50 °C [Fig. 2(a)],  $a/b$  and  $a/c$  domain walls coexist. The  $a/b$  domain walls, signaled with dashed lines, reveal a domain periodicity of  $(500 \pm 50) \text{ nm}$  for this



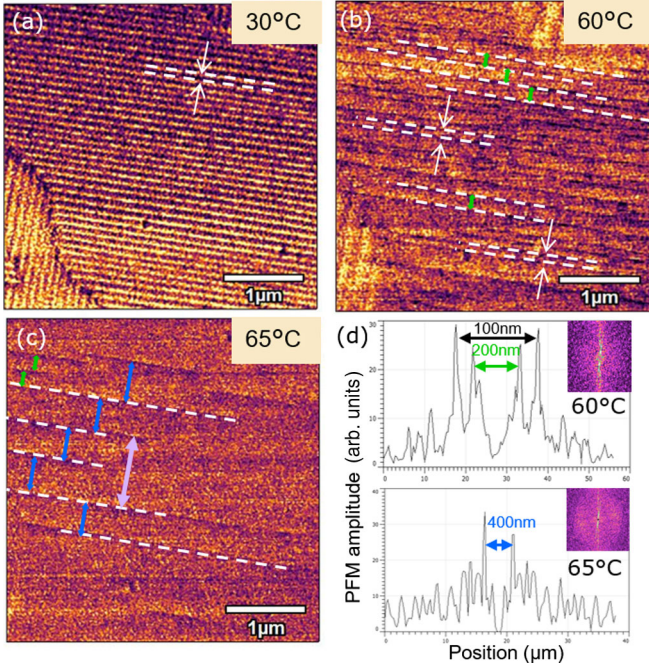


FIG. 3. Amplitude of the LPMF signal of a 90 nm thick BaTiO<sub>3</sub> film on a NdScO<sub>3</sub> substrate measured during heating at (a) 30 °C, (b) 60 °C, and (c) 65 °C. (d) FFT of the images in (b) and (c), from which the domain period is determined. The basic domain width  $w_0 = 110$  nm is indicated by the white arrows in (a) and (b). Other detected periodicities are  $w = 2w_0 = 200$  nm (green) in (b) and (c), as well as  $w = 4w_0 = 400$  nm (blue). A domain with size  $w = 8w_0 = 800$  nm (violet) is also observed in (c).

170 nm thick film. The periodicity values are obtained by performing the fast Fourier transform (FFT) of the LPMF images (see Sec. II of the Supplemental Material [35] for details). Further cooling down to 30 °C [Fig. 2(b)] shows new  $b$  domains appearing halfway between the existing domain walls, halving the domain periodicity to  $(250 \pm 20)$  nm. This value is, in turn, approximately double that found at room temperature, after the sample has equilibrated for several hours and the high-temperature domain configuration has disappeared [see the inset of Fig. 1(a)]. Thus, two sequential periodicity halving events take place during the transition from the  $a/c$  to the  $a/b$  domain configuration on cooling.

A similar mechanism, albeit shifted in temperature due to thermal hysteresis, is observed when heating the samples through the phase transition, as shown in Fig. 3. The transition from  $a/b$  to  $a/c$  domains is followed on heating from 30 °C to 70 °C at 5 °C steps. The initial  $a/b$  domain periodicity at 30 °C is  $w_0 = 100$  nm for a sample with a thickness of 90 nm [Fig. 3(a)]. The domain walls start to rearrange, and at 60 °C [Fig. 3(b)], domains with  $w = 2w_0$  are visible, as indicated by the green arrows. With increasing temperature up to 65 °C [Fig. 3(c)],  $w = 4w_0$  becomes the most abundant period (blue arrows) [see the FFT in Fig. 3(d)]. In addition, a domain with a size of  $w = 8w_0$  (violet arrow) can be observed within the area of the image

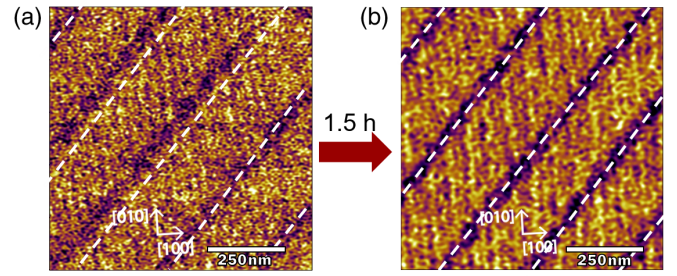


FIG. 4. LPMF amplitude images of a 170 nm thick BaTiO<sub>3</sub> film. (a) Five different  $b$  domains (darker diagonal bands) with different separations ( $a$ -domain widths). (b) After waiting for 1.5 h, the domain walls rearrange towards achieving a periodic configuration. The dashed lines signal the position of the  $b$  domains in the ideal periodic case.

(See Fig. S2 in the Supplemental Material [35] for the FFT of all three images). So the transition to the  $a/c$  phase takes place by sequentially annihilating one every other  $b$  domain, and, thus, the apparent domain periodicities follow a Cantor set sequence with  $w = 2^n w_0$  [52]. Prefractal domain patterns following Cantor set sequences have been observed in ferroelectrics under electric field [53]. Subsequent periodicity-doubling events in these material have also been observed by reciprocal space mapping (see Sec. IV of the Supplemental Material [35] for further details).

Our experiments also show the self-repairing of “wrongly” nucleated domain walls, indicating that the center of existing domains is the equilibrium position for new domains. Figure 4(a) shows  $b$  domains right after their formation, displaying unequal widths, probably due to pinning by the local defect structure. However, the elastic forces in this situation lead to a movement of the  $b$  domains with respect to each other to reach a position equidistant between the neighboring  $b$  domains [Fig. 4(b)]. It is well known that defects act as preferred nucleation points for new domains [11,43], as observed in Fig. 2(a), where a defect (two  $a/c$  domains merging into one) close to the center of an  $a$  domain induces the bending of the new wall in Fig. 2(b). Because of the random nature of these defects, we have occasionally observed deviations from the apparent  $2^n$  domain evolution law.

Phase-field simulations are performed using the time-dependent Ginzburg-Landau equations for BaTiO<sub>3</sub> under strain (see Sec. II B of the Supplemental Material [35] for details), and the results are shown in Fig. 5. It is seen that the alternating pseudo- $a/b$  phase appears at low temperatures, and an  $a/c$  tetragonal structure predominates at high temperatures. Figure 5(a) shows that the domain structure of the high-temperature phase,  $a/c$ , agrees with the experimental observations previously captured by Everhardt *et al.* [33] with  $\{101\}$  domain walls (thus, consistent with the  $[010]$  projections on the PFM images). These simulations also demonstrate the change in domain wall orientation from  $\{101\}$  to  $\{110\}$ , also consistent with

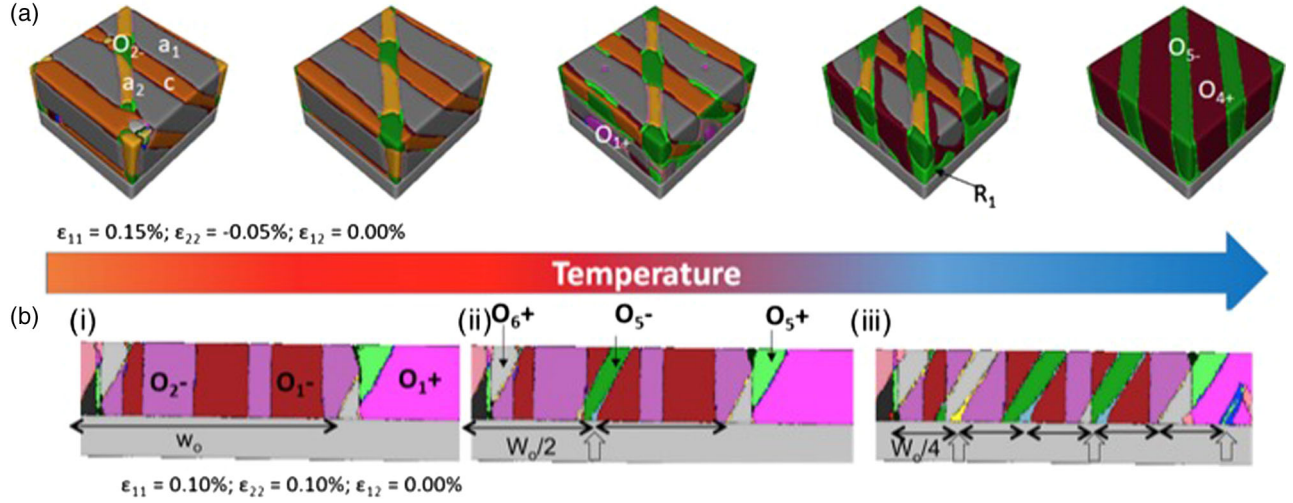


FIG. 5. (a) Three-dimensional and (b) two-dimensional domain structures generated by the phase-field method, indicating the misfit strain conditions that led to their formation. In (a), as the temperature decreases from 100 °C to 25 °C, a change in domain wall orientation from  $\{101\}$  to  $\{110\}$  takes place signaling the phase transition. It is also apparent that the new domains form at the halfway point between the original domain walls. In (b), subsequent nucleation of a new domain halfway between existing domain walls (shown by the open vertical arrows) is also shown to take place as the temperature decreases from (i) 80 °C to (ii) 60 °C and to (iii) 25 °C. Domain notation is as follows:  $a_1 = (P_0, 0, 0)$ ,  $a_2 = (0, P_0, 0)$ ,  $c = (0, 0, P_0)$ ,  $O_{1+} = (P_0, P_0, 0)$ ,  $O_{1-} = (-P_0, -P_0, 0)$ ,  $O_{2+} = (P_0, -P_0, 0)$ ,  $O_{2-} = (-P_0, P_0, 0)$ ,  $O_{4+} = (P_0, 0, -P_0)$ ,  $O_{5+} = (0, P_0, P_0)$ ,  $O_{5-} = (0, -P_0, -P_0)$ ,  $O_{6+} = (0, P_0, -P_0)$ ,  $O_{6-} = (0, -P_0, P_0)$ , and  $R_1 = (P_0, -P_0, -P_0)$ .

PFM observations, with the “new” (orthorhombic) domains forming in the middle of the “old” (tetragonal) domains. An analysis of the phase-field simulation results in a  $\beta$  coefficient of  $\beta = 7 \text{ nm}^{1/2}$  at high temperature and  $\beta = 10 \text{ nm}^{1/2}$  at low temperature, supporting our experimental observations in Fig. 1.

Investigation of the elastic energies agrees with the experimental observation of stress relaxation being achieved by the formation of new domains at the center of old domains. To increase the simulation areas, we have also performed 2D simulations [see Fig. 5(b)]. In this case, the orientation of the polarization in the two phases does not fully agree with the experiment due to the simplicity of the model, but successive nucleation of new domains halfway between existing domain walls is clearly observed as the temperature is decreased. In addition, it is shown that the new domains nucleate near the film-substrate interface, at the  $90^\circ$  (100) domain wall and along the  $\langle 110 \rangle$  directions.

Thus, periodicity changes take place by the formation of new stress-relieving elements (singularities) exactly in the center of the old domains, as already predicted by dynamic pattern formation [54,55]. In the current measurements, a new  $b$  domain (thus, a pair of domain walls) conforms such singularity, but other types such as single domain walls, dislocations, cracks, etc., are governed by similar physics. In the case of ferroelastic domains, increasing the strain (e.g., by decreasing the temperature) would repeat the process between a first-generation singularity and a second-generation singularity, and so on.

More generally, in addition to boundary conditions and the effect of substrates, effective interactions between domain walls and evolution of domain wall structures can come from other physical processes. If several order parameters are activated to generate a domain wall, the energy landscape is complex with several minima, which combine to define the domains and the wall structures. Lateral extensions of domain walls would favor the wall-wall interactions and such phenomena have been explored in biquadratic or linear quadratic coupling between order parameters [56–61]. Atomistic approaches are very limited [62,63] at this time, and no firm conclusions can be reached for direct interactions. If no such wall-wall interaction existed and no external constraints occurred, then the pattern energy density would depend only on the total number of domain walls and their self-energy.

Periodicity can also originate from nucleation. Domains nucleate from the surface or an interface and the nucleation centers repel each other. The periodicity and deviations from a periodic array stem from the mistakes in distribution of nucleation sites, which would often form Cantor sets leading to phenomena like period doubling and local periodicity disorder [64–66]. Finally, we mention that, in free crystals, periodicity of domain walls, period doubling, and disorder can be induced by the sideways movement of domains in terms of front propagation [55,60,67,68].

Recent work [69–71] shows that, during the ferroelectric phase transition at 120 °C, BaTiO<sub>3</sub> crystals display transient intersections between polar ferroelastic or ferroelectric  $90^\circ$  walls and the (001) surface that are electrically charged and



persist up to temperatures above  $T_C$ , while the bulk has already transformed into the cubic phase. Interestingly, a sequential period halving evolution in which some domains are missing during the cooldown process, most likely due to the local presence of other types of defects taking care of the stress relaxation, can explain the *discretization* of domain sizes that we have detected in various ferroelastic materials [48,49,72–74] (see Sec. V of the Supplemental Material [35]).

In conclusion, we directly observe in this Letter spatial period-doubling or halving sequences consistent with those found as part of the clock-model calculations [75]. This behavior belongs to a class of scaling phenomena known as period-doubling cascades that are mathematically investigated by means of bifurcation theory and characterize systems at the “edge of chaos.” Even though a link with spatially modulated phases of matter has been made [1], spatial period-doubling cascades had not yet been observed experimentally. Thus, our observation of domain periodicity halving should not be exclusive of the system under investigation, but it represents a more general mechanism of transformation in materials with competing periodic structures.

The authors are grateful to Janusz Przeslawski, Marty Gregg, Jim Scott, and Yachin Yvry for the useful discussions. A. S. E., S. D., and B. N. acknowledge financial support from the alumni organization of the University of Groningen, De Aduarderking (Ubbo Emmius Fonds). Parts of this research were carried out at the light source Petra III at DESY, a member of the Helmholtz Association (HGF). G. C. and N. D. acknowledge Projects No. FIS2015-73932-JIN and No. MAT2016-77100-C2-1-P from the Spanish MINECO and Project No. 2017-SGR-579 from the Generalitat de Catalunya. All work at ICN2 is also supported by the Severo Ochoa Program (Grant No. SEV-2017-0706). The work at Penn State is supported by the U.S. Department of Energy, Office of Basic Energy Sciences, Division of Materials Sciences and Engineering, under Award No. FG02-07ER46417 (J. A. Z. and L.-Q. C.) and, partially, by a graduate fellowship from the 3M Company (J. A. Z.).

E. A. S. and D. S. contributed equally to this work.

\*Present address: Materials Science Division, Lawrence Berkeley National Laboratory, Berkeley, California 94720, USA.

†s.damerio@rug.nl

‡b.noheda@rug.nl

- [1] M. H. Jensen and P. Bak, *Phys. Scr. T* **T9**, 64 (1985).
- [2] W. Selke, *Phys. Rep.* **170**, 213 (1988).
- [3] Z. Hong, A. R. Damodaran, F. Xue, S. L. Hsu, J. Britson, A. K. Yadav, C. T. Nelson, J. J. Wang, J. F. Scott, L. W. Martin, R. Ramesh, and L. Q. Chen, *Nano Lett.* **17**, 2246 (2017).
- [4] P. Shafer, P. García-Fernández, P. Aguado-Puente, A. R. Damodaran, A. K. Yadav, C. T. Nelson, S.-L. Hsu, J. C. Wojdeł, J. Íñiguez, L. W. Martin, E. Arenholz, J. Junquera, and R. Ramesh, *Proc. Natl. Acad. Sci. U.S.A.* **115**, 915 (2018).
- [5] E. K. Salje, *Annu. Rev. Mater. Res.* **42**, 265 (2012).
- [6] A. L. Roitburd, *Phys. Status Solidi (a)* **37**, 329 (1976).
- [7] W. Pompe, X. Gong, Z. Suo, and J. S. Speck, *J. Appl. Phys.* **74**, 6012 (1993).
- [8] N. A. Pertsev and A. G. Zembilgotov, *J. Appl. Phys.* **78**, 6170 (1995).
- [9] G. Catalan, J. Seidel, R. Ramesh, and J. F. Scott, *Rev. Mod. Phys.* **84**, 119 (2012).
- [10] I. A. Lukyanchuk, A. Schilling, J. M. Gregg, G. Catalan, and J. F. Scott, *Phys. Rev. B* **79**, 144111 (2009).
- [11] A. K. Tagantsev, L. E. Cross, and J. Fousek, *Domains in Ferroic Crystals and Thin Films* (Springer Science+Business Media, New York, 2011).
- [12] A. H. G. Vlooswijk, B. Noheda, G. Catalan, A. Janssens, B. Barcones, G. Rijnders, D. H. A. Blank, S. Venkatesan, B. Kooi, and J. T. M. de Hosson, *Appl. Phys. Lett.* **91**, 112901 (2007).
- [13] L. Feigl, P. Yudin, I. Stolichnov, T. Sluka, K. Shapovalov, M. Mtebwa, C. S. Sandu, X.-K. Wei, A. K. Tagantsev, and N. Setter, *Nat. Commun.* **5**, 4677 (2014).
- [14] J. F. Scott, D. M. Evans, R. S. Katiyar, R. G. P. McQuaid, and J. M. Gregg, *J. Phys. Condens. Matter* **29**, 304001 (2017).
- [15] D. D. Fong, G. B. Stephenson, S. K. Streiffer, J. A. Eastman, O. Auciello, P. H. Fuoss, and C. Thompson, *Science* **304**, 1650 (2004).
- [16] G. Catalan, A. Lubk, A. H. G. Vlooswijk, E. Snoeck, C. Magen, A. Janssens, G. Rispens, G. Rijnders, D. H. A. Blank, and B. Noheda, *Nat. Mater.* **10**, 963 (2011).
- [17] P. Gao, J. Britson, C. T. Nelson, J. R. Jokisaari, C. Duan, M. Trassin, S.-H. Baek, H. Guo, L. Li, Y. Wang, Y.-H. Chu, A. M. Minor, C.-B. Eom, R. Ramesh, L.-Q. Chen, and X. Pan, *Nat. Commun.* **5**, 3801 (2014).
- [18] P. Gao, J. Britson, J. R. Jokisaari, C. T. Nelson, S.-H. Baek, Y. Wang, C.-B. Eom, L.-Q. Chen, and X. Pan, *Nat. Commun.* **4**, 2791 (2013).
- [19] A. I. Khan, X. Marti, C. Serrao, R. Ramesh, and S. Salahuddin, *Nano Lett.* **15**, 2229 (2015).
- [20] J. C. Agar, A. R. Damodaran, M. B. Okatan, J. Kacher, C. Gammer, R. K. Vasudevan, S. Pandya, R. V. K. Mangalam, G. A. Velarde, S. Jesse, N. Balke, A. M. Minor, S. V. Kalinin, and L. W. Martin, *Nat. Mater.* **15**, 549 (2016).
- [21] L. J. McGilly, T. L. Burnett, A. Schilling, M. G. Cain, and J. M. Gregg, *Phys. Rev. B* **85**, 054113 (2012).
- [22] M. Takashige, S. Hamazaki, Y. Takahashi, F. Shimizu, and T. Yamaguchi, *Jpn. J. Appl. Phys.* **38**, 5686 (1999).
- [23] Y. Ivry, C. Durkan, D. Chu, and J. F. Scott, *Adv. Funct. Mater.* **24**, 5567 (2014).
- [24] Y. Ivry, D. Chu, J. F. Scott, and C. Durkan, *Adv. Funct. Mater.* **21**, 1827 (2011).
- [25] R. J. Harrison, S. A. T. Redfern, A. Buckley, and E. K. H. Salje, *J. Appl. Phys.* **95**, 1706 (2004).
- [26] R. J. Harrison, S. A. T. Redfern, and E. K. H. Salje, *Phys. Rev. B* **69**, 144101 (2004).

- [27] A. Schilling, A. Kumar, R. G. P. McQuaid, A. M. Glazer, P. A. Thomas, and J. M. Gregg, *Phys. Rev. B* **94**, 024109 (2016).
- [28] A. L. Tolstikhina, R. V. Gainutdinov, N. V. Belugina, A. K. Lashkova, A. S. Kalinin, V. V. Atepalikhin, V. V. Polyakov, and V. A. Bykov, *Physica (Amsterdam)* **550B**, 332 (2018).
- [29] G. Sheng, J. X. Zhang, Y. L. Li, S. Choudhury, Q. X. Jia, Z. K. Liu, and L. Q. Chen, *Appl. Phys. Lett.* **93**, 232904 (2008).
- [30] L. Q. Chen, *J. Am. Ceram. Soc.* **91**, 1835 (2008).
- [31] Y. Li, S. Y. Hu, Z. K. Liu, and L. Q. Chen, *Appl. Phys. Lett.* **81**, 427 (2002).
- [32] Y. L. Li and L. Q. Chen, *Appl. Phys. Lett.* **88**, 072905 (2006).
- [33] A. S. Everhardt, S. Matzen, N. Domingo, G. Catalan, and B. Noheda, *Adv. Electron. Mater.* **2**, 1500214 (2016).
- [34] V. G. Koukhar, N. A. Pertsev, and R. Waser, *Phys. Rev. B* **64**, 214103 (2001).
- [35] See Supplemental Material at <http://link.aps.org/supplemental/10.1103/PhysRevLett.123.087603>, which includes Refs. [[6–8,31,33,34,36–50]], for additional information.
- [36] Y. Li, S. Hu, Z. Liu, and L. Chen, *Acta Mater.* **50**, 395 (2002).
- [37] A. S. Everhardt, T. Denneulin, A. Grünebohm, Y.-T. Shao, P. Ondrejčovič, F. Borodavka, I. Gregora, S. Zhou, N. Domingo, N. Catalan, J. Hlinka, J.-M. Zuo, S. Matzen, and B. Noheda, [arXiv:1907.09709](https://arxiv.org/abs/1907.09709).
- [38] K. J. Choi, M. Biegalski, Y. L. Li, A. Sharan, J. Schubert, R. Uecker, P. Reiche, Y. B. Chen, X. Q. Pan, V. Gopalan, L.-Q. Chen, D. G. Schlom, and C. B. Eom, *Science* **306**, 1005 (2004).
- [39] R. Uecker, B. Velickov, D. Klimm, R. Bertram, M. Bernhagen, M. Rabe, M. Albrecht, R. Fornari, and D. Schlom, *J. Cryst. Growth* **310**, 2649 (2008).
- [40] L. Chen and J. Shen, *Comput. Phys. Commun.* **108**, 147 (1998).
- [41] G. Catalan, I. Lukyanchuk, A. Schilling, J. M. Gregg, and J. F. Scott, *J. Mater. Sci.* **44**, 5307 (2009).
- [42] G. Catalan, J. F. Scott, A. Schilling, and J. M. Gregg, *J. Phys. Condens. Matter* **19**, 022201 (2007).
- [43] A. Schilling, T. B. Adams, R. M. Bowman, J. M. Gregg, G. Catalan, and J. F. Scott, *Phys. Rev. B* **74**, 024115 (2006).
- [44] A. Schilling, R. M. Bowman, C. Catalan, J. F. Scott, and J. M. Gregg, *Nano Lett.* **7**, 3787 (2007).
- [45] M. Mtebwa, L. Feigl, P. Yudin, L. J. McGilly, K. Shapovalov, A. K. Tagantsev, and N. Setter, *Appl. Phys. Lett.* **107**, 142903 (2015).
- [46] D. Vul and E. Salje, *Physica (Amsterdam)* **253C**, 231 (1995).
- [47] G. Catalan, H. Béa, S. Fusil, M. Bibes, P. Paruch, A. Barthélémy, and J. F. Scott, *Phys. Rev. Lett.* **100**, 027602 (2008).
- [48] O. Nesterov, S. Matzen, C. Magen, A. H. G. Vlooswijk, G. Catalan, and B. Noheda, *Appl. Phys. Lett.* **103**, 142901 (2013).
- [49] A. Roelofs, N. A. Pertsev, R. Waser, F. Schlaphof, L. M. Eng, C. Ganpule, V. Nagarajan, and R. Ramesh, *Appl. Phys. Lett.* **80**, 1424 (2002).
- [50] A. Venkatesan, S. Parthasarathy, and M. Lakshmanan, *Chaos Solitons Fractals* **18**, 891 (2003).
- [51] J. J. Wang, P. P. Wu, X. Q. Ma, and L. Q. Chen, *J. Appl. Phys.* **108**, 114105 (2010).
- [52] This is an apparent rule because it ignores the finite width of the *b* domains not properly resolved in PFM images.
- [53] T. Ozaki, K. Fujii, and J. Ohgami, *J. Phys. Soc. Jpn.* **64**, 2282 (1995).
- [54] E. K. H. Salje, *J. Phys. Condens. Matter* **5**, 4775 (1993).
- [55] I. Tsatskis, E. K. H. Salje, and V. Heine, *J. Phys. Condens. Matter* **6**, 11027 (1994).
- [56] J. M. Ball and E. C. M. Crooks, *Calc. Var.* **40**, 501 (2011).
- [57] S. Conti, S. Müller, A. Poliakovsky, and E. K. H. Salje, *J. Phys. Condens. Matter* **23**, 142203 (2011).
- [58] B. Houchmandzadeh, J. Lajzerowicz, and E. Salje, *J. Phys. Condens. Matter* **3**, 5163 (1991).
- [59] B. Houchmandzadeh, J. Lajzerowicz, and E. Salje, *J. Phys. Condens. Matter* **4**, 9779 (1992).
- [60] B. Houchmandzadeh, J. Lajzerowicz, and E. Salje, *Phase Transit.* **38**, 77 (1992).
- [61] H. Pöttker and E. K. H. Salje, *J. Phys. Condens. Matter* **26**, 342201 (2014).
- [62] E. K. H. Salje, *Phase Transitions in Ferroelastic and Co-Elastic Crystals: An Introduction for Mineralogists, Material Scientists, and Physicists* (Cambridge University Press, Cambridge, England, 1993).
- [63] A. M. Bratkovsky and A. P. Levanyuk, *Phys. Rev. Lett.* **86**, 3642 (2001).
- [64] L. Zuberger, *J. Math. Anal. Appl.* **474**, 143 (2019).
- [65] L. Sun, C. Fang, Y. Song, and Y. Guo, *J. Phys. Condens. Matter* **22**, 445303 (2010).
- [66] T. Ozaki and J. Ohgami, *J. Phys. Condens. Matter* **7**, 1711 (1995).
- [67] W. van Saarloos and P. Hohenberg, *Physica (Amsterdam)* **56D**, 303 (1992).
- [68] G. T. Dee and W. van Saarloos, *Phys. Rev. Lett.* **60**, 2641 (1988).
- [69] C. Mathieu, C. Lubin, G. Le Doueff, M. Cattelan, P. Gemeiner, B. Dkhil, E. K. Salje, and N. Barrett, *Sci. Rep.* **8**, 13660 (2018).
- [70] N. Barrett, J. Dionot, D. Martinotti, E. K. Salje, and C. Mathieu, *Appl. Phys. Lett.* **113**, 022901 (2018).
- [71] G. F. Nataf, M. Guennou, J. Kreisel, P. Hicher, R. Haumont, O. Aktas, E. K. Salje, L. Torteche, C. Mathieu, D. Martinotti, and N. Barrett, *Phys. Rev. Mater.* **1**, 074410 (2017).
- [72] C. S. Ganpule, V. Nagarajan, H. Li, A. S. Ogale, D. E. Steinhauer, S. Aggarwal, E. Williams, R. Ramesh, and P. De Wolf, *Appl. Phys. Lett.* **77**, 292 (2000).
- [73] S. Y. Hu, Y. L. Li, and L. Q. Chen, *J. Appl. Phys.* **94**, 2542 (2003).
- [74] V. Nagarajan, C. S. Ganpule, H. Li, L. Salamanca-Riba, A. L. Roytburd, E. D. Williams, and R. Ramesh, *Appl. Phys. Lett.* **79**, 2805 (2001).
- [75] P. D. Scholten and D. R. King, *Phys. Rev. B* **53**, 3359 (1996).